Supplementary Material:

Air quality in the middle and lower reaches of the Yangtze River channel: A cruise campaign

Zhong Li[1], Chunlin Li[1,2], Xingnan Ye[1], Hongbo Fu[1], Lin Wang[1], Xin Yang[1], Xinke Wang[3]， Zhuohui Zhao[4], Haidong Kan[4], Abdelwahid Mellouki[5], Jianmin Chen[1,4,*]

[1] *Shanghai Key Laboratory of Atmospheric Particle Pollution and Prevention, Fudan Tyndall Center, Department of Environmental Science & Engineering, Institute of Atmospheric Sciences, Fudan University, Shanghai 200433, China*

[2] *Department of Earth and Planetary Sciences,Weizmann Institute of Science*

[3] *Univ Lyon, Université Claude Bernard Lyon 1 CNRS, IRCELYON, F-69626, Villeurbanne, France*

[4] *School of Public Health, Fudan University, Shanghai 200032, China*

[5] *Institut de Combustion, Aérothermique, Réactivité et Environnement, CNRS, 45071 Orléans cedex 02, France*

[*]Correspondence to*:* **Jianmin Chen (jmchen@fudan.edu.cn)**

1 Meteorology pattern over the cruise

The MLYP region is located in East Asia Monsoon Region (China type), of which has a clear seasonal shift of the prevailing wind between in winter and summer. As shown in Figure S3, West Pacific Subtropical High (WPSH) control the south China in winter, while a cold high pressure formed in the north region of China during the period. During the sampling periods, WPSH was constantly squeezed further to south and ocean. The YRC region is completely situated between high pressure ridge and trough, thus northwest winds are dominant, as verified by two cold fronts on 25 November and 2 December in 2015, respectively. Besides, a low-pressure system formed in central China from 28 to 30 November, which was characterized by relative low wind speed and even stagnant air-mass, of which made a great contribution to the formation of the haze pollution (Huang et al., 2014;Huang et al., 2012).

The detailed meteorological information, including temperature (T), RH, pressure, wind speed (WS) and wind direction (WD) were monitored by an automatic meteorological station (HydroMet^{TM}, Vaisala) placed on the front of the vessel. The true wind, i.e., a vector wind with a speed referenced to the fixed earth and a direction referenced to true north, was established by the platform-relative wind to ship and vessel speed, which was calculated directly from Global Positioning System (GPS) records (Smith et al., 1999). T and RH showed greatly changes during the survey, range from 1.05-18.90 ℃ and 26.90-99.00%, respectively. The surface WD was relative constant and WS was low in the most time during YRC, and the mean speed of 3.10 ± 0.99 m/s were measured. There were two sharp reduction of T and RH on 25 November and 2 December. When the cold front arrived, WS increases from 2 m/s up to 10 m/s.

Table S1. Emission factors of 11 metals from different fuel combustion (mg/kg) measured in our lab (Wu et al., 2017).

	Light diesel oil	Marine heavy diesel oil	93 octane petrol	97 octane petrol
As	7.91 ± 1.03	1.77 ± 0.51	2.55 ± 0.31	1.30 ± 0.17
Fe	7.87 ± 1.12	12.28 ± 2.85	18.30 ± 1.39	20.07 ± 0.48
Al	4.39 ± 1.26	1.25 ± 0.35	0.33 ± 0.00	0.21 ± 0.00
Mn	2.62 ± 0.45	2.47 ± 0.70	0.57 ± 0.24	0.41 ± 0.03
Pb	1.13 ± 0.15	12.39 ± 0.65	ND	ND
Cr	0.73 ± 0.08	0.22 ± 0.09	0.24 ± 0.05	0.16 ± 0.10
Zn	0.43 ± 0.05	5.46 ± 1.32	0.05 ± 0.02	0.09 ± 0.03
Cu	0.40 ± 0.16	0.10 ± 0.03	0.40 ± 0.00	0.27 ± 0.12
V	ND	0.48 ± 0.11	ND	ND
Cd	ND	ND	ND	ND
Ni	0.24 ± 0.02	0.39 ± 0.06	0.07 ± 0.01	0.21 ± 0.04
TMs	25.72 ± 4.32	36.81 ± 6.67	22.51 ± 2.02	22.72 ± 0.97

Table S2. The average and maximum contribution of SO_4^{2-}, NO_3^-, OC and $PM_{2.5}$ from ship plume estimated by a lower limit ratio.

ship emission contribution	$PM_{2.5}$	$(OC/V)_{min} = 142$	$(NO_3^-/V)_{min} = 228$	$(SO_4^{2-}/V)_{min} = 127$
Average (μg m^{-3})	8.46	3.63	2.22	1.38
Percent (%)	6.73	23.84	16.1	33.9
Maximum (μg m^{-3})	58.9	15.21	13.8	4.09
Percent (%)	52.3	22.39	13.7	8.55

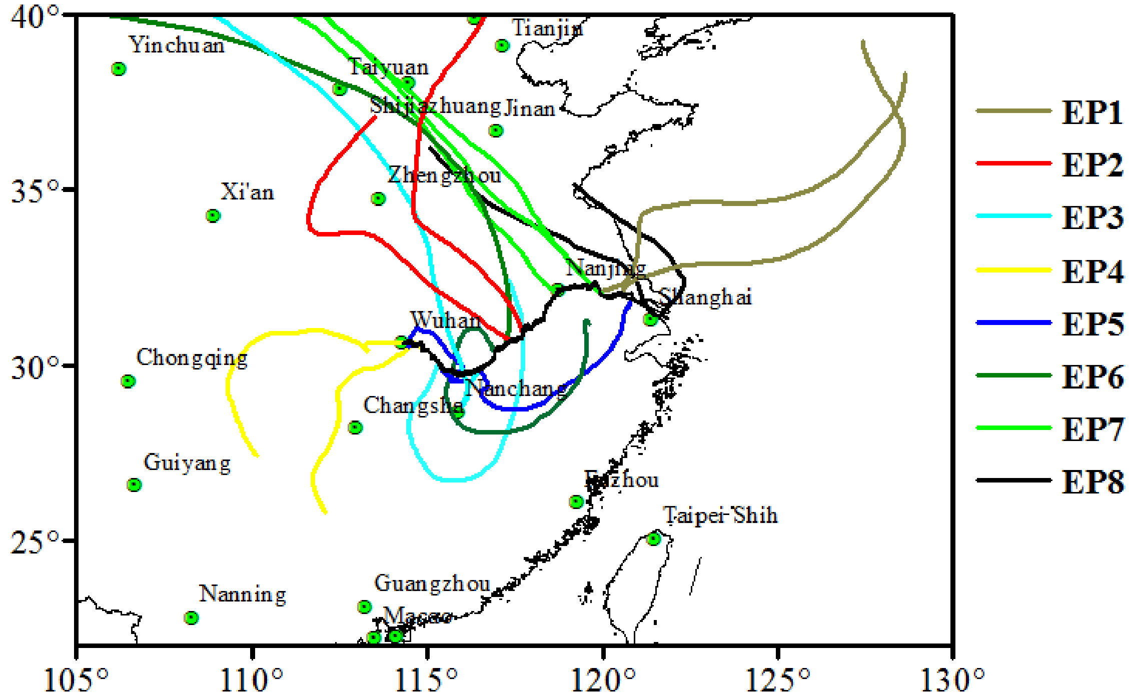

Figure S1. Ship route and 3-day back trajectories arriving at 500 m above sea level.

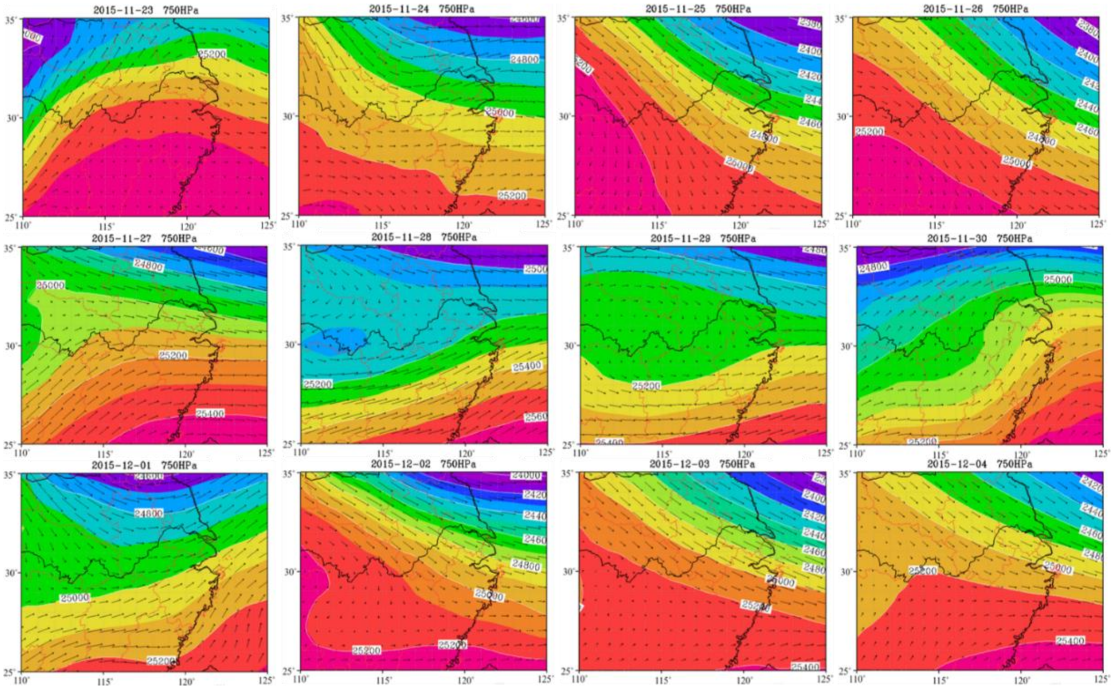

Figure S2. The average geopotential height field (white lines) and wind field (blank vector) for 750 hPa for each day during YRC.

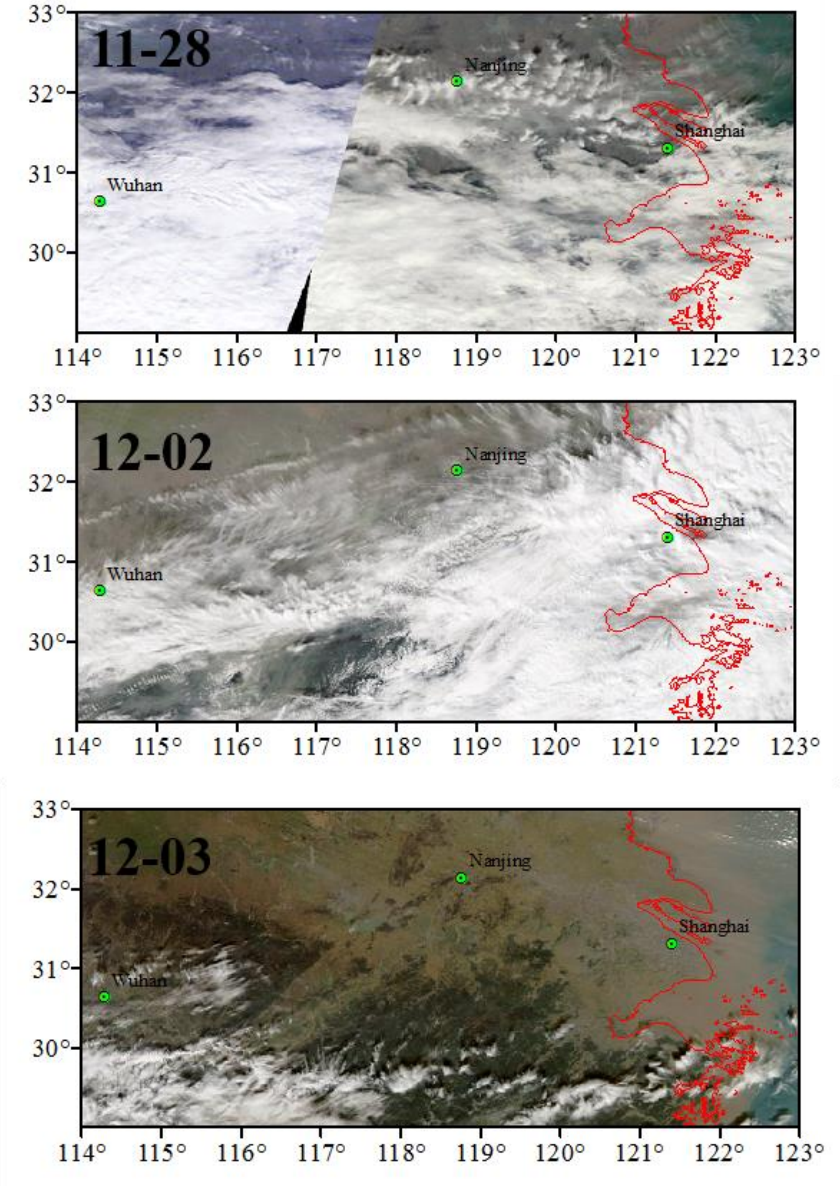

Figure S3. MODIS true-color imagery on 28 November, 2 and 3 December in 2015.

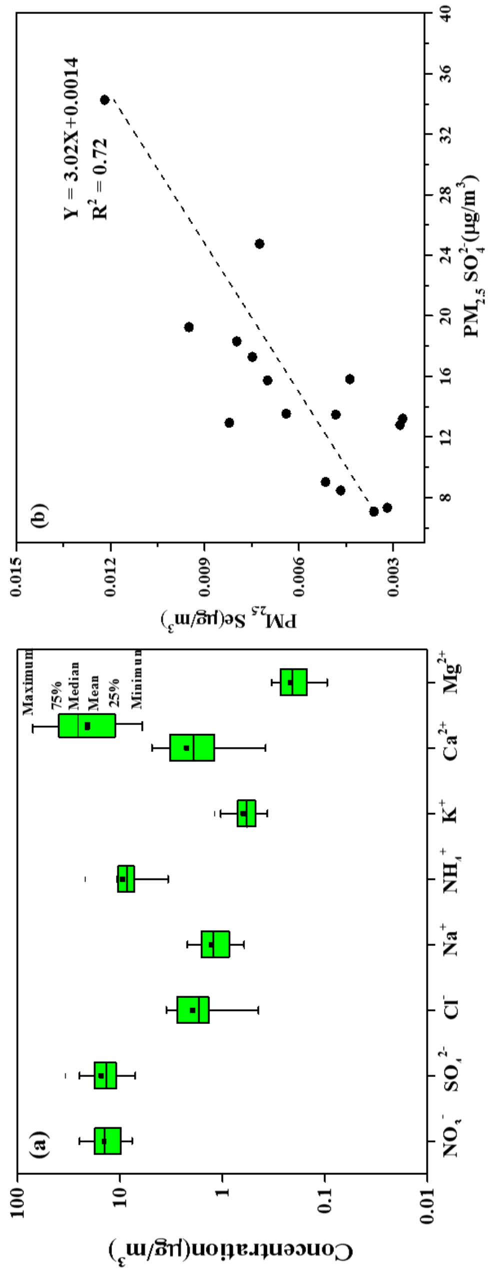

Figure S4. (a) average mass concentration of the main soluble ions along YRC; (b) the linear correlation between Se and SO_4^{2-} in $PM_{2.5}$.

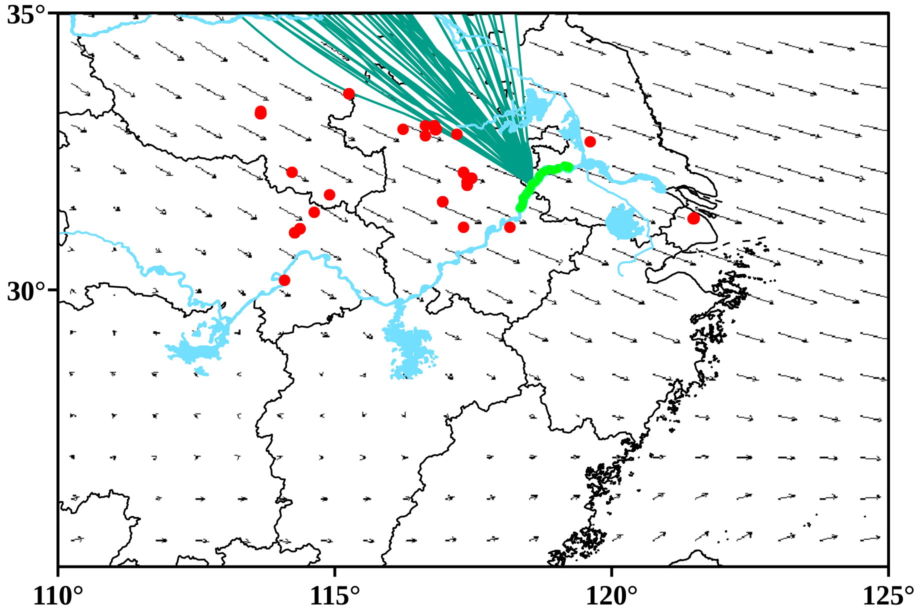

Figure S5. Mean wind vectors for sample #12 beginning at 18:00 LST and ending at 06:00 LST next day. Green line is the route for this sample. Red dots represent the FIRMS's fire points.

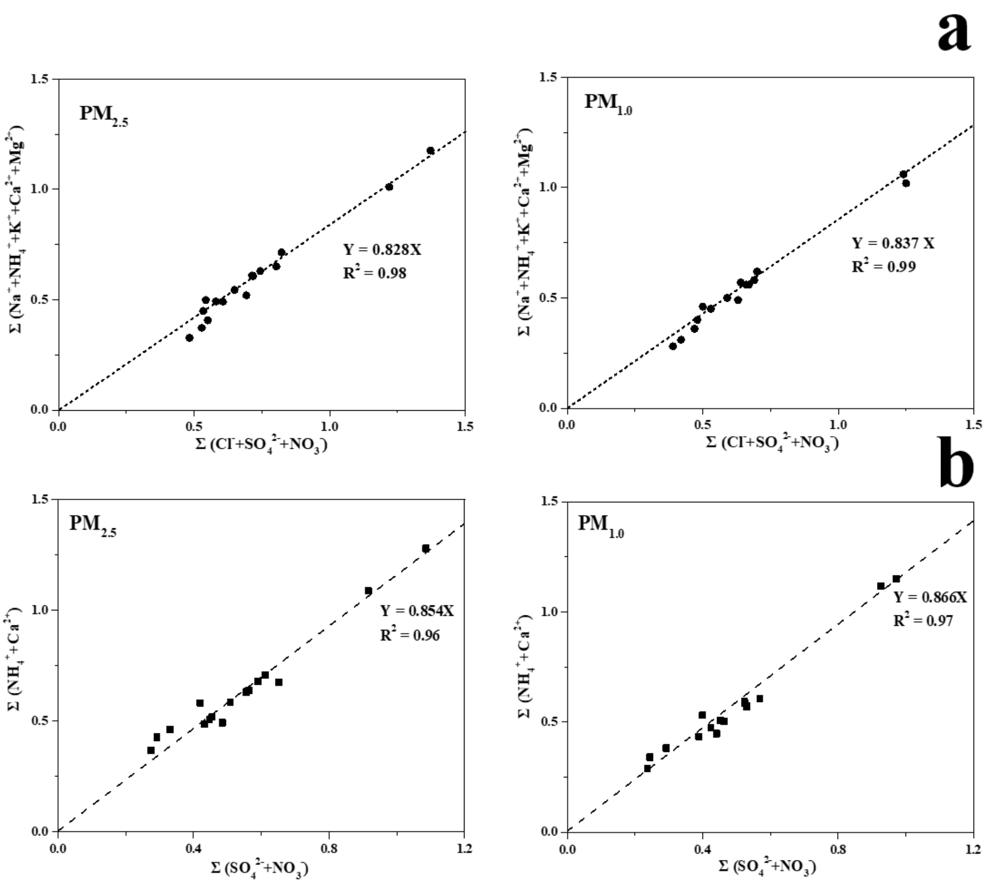

Figure S6. (a) The ion balance; (b) The correlation between the equivalent concentrations of $[SO_4^{2-} + NO_3^-]$ and $[NH_4^+ + Ca^{2+}]$ in the present study (μ eq m^{-3}).

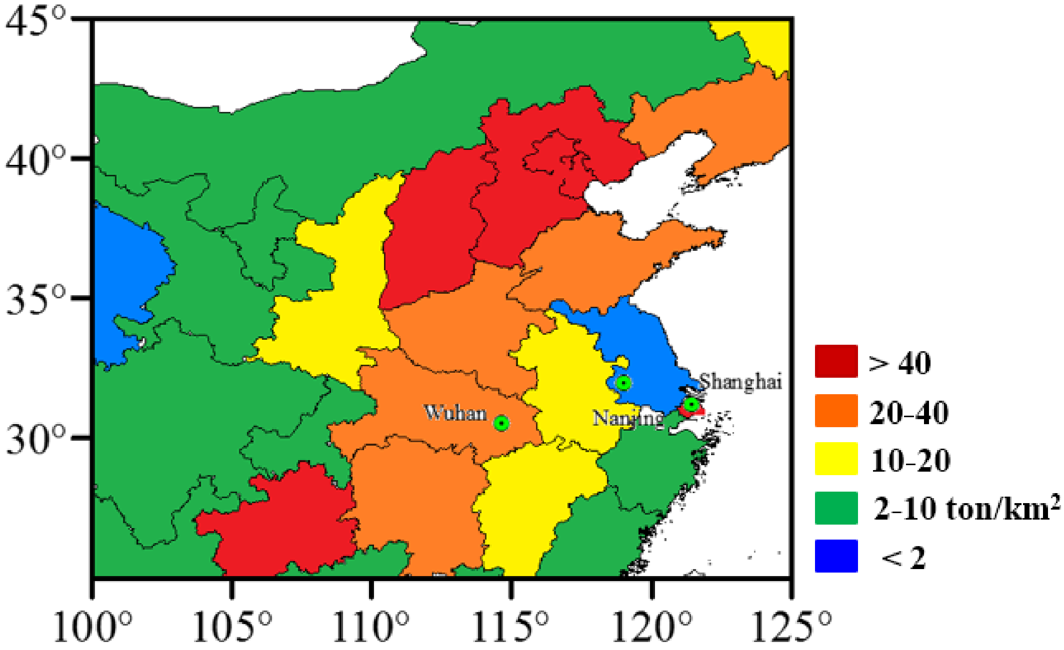

Figure S7. Residential coal consumption in China in 2015 (source: China energy statistical yearbook (NBSC, 2016)).

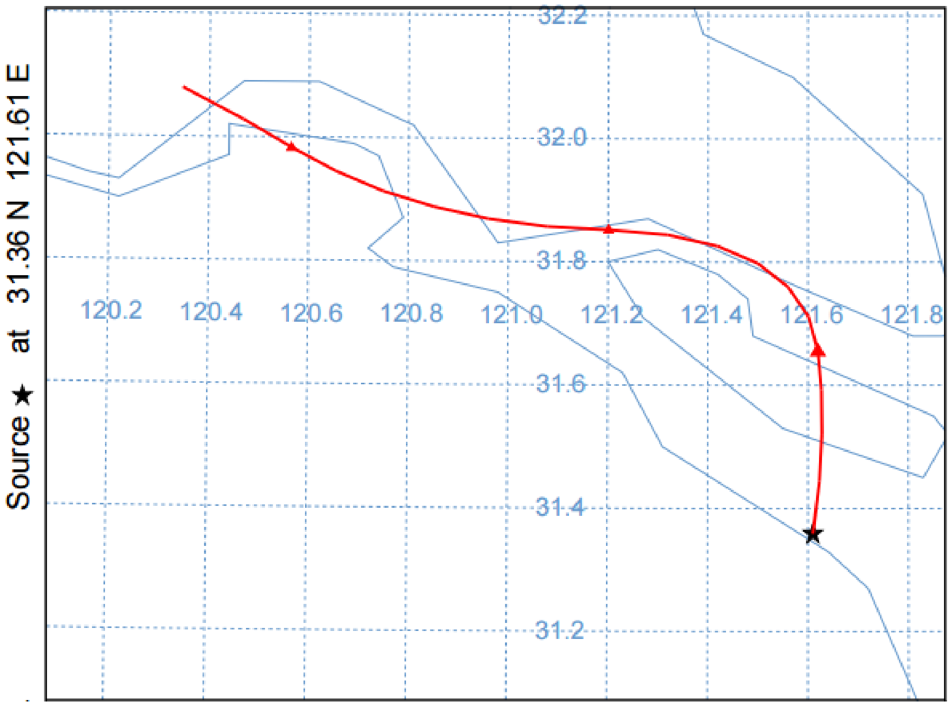

Figure S8. 18-hours back trajectories arriving at 500 m above sea level during the sample 16.

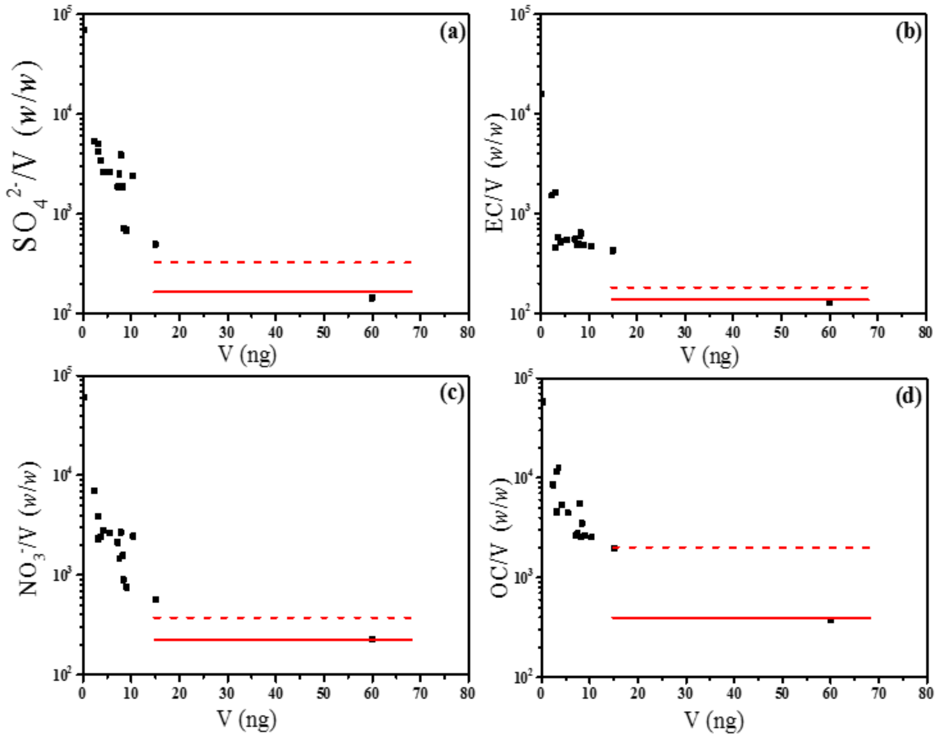

Figure S9. Scatter ration of (a) SO_4^{2-}/V, (b) NO_3^-/V, (c) EC/V and (d) OC/V along YRC. The red dashed line represented average ratio and solid line express the minimum ratio (average minus one standard deviation) for the sample with V > 15 ng/m^3.

Reference

Huang, K., Zhuang, G., Lin, Y., Fu, J. S., Wang, Q., Liu, T., Zhang, R., Jiang, Y., Deng, C., and Fu, Q.: Typical types and formation mechanisms of haze in an Eastern Asia megacity, Shanghai, Atmos. Chem. Phys., 12, 105,doi: 10.5194/acp-12-105-2012, 2012.

Huang, R.-J., Zhang, Y., Bozzetti, C., Ho, K.-F., Cao, J.-J., Han, Y., Daellenbach, K. R., Slowik, J. G., Platt, S. M., and Canonaco, F.: High secondary aerosol contribution to particulate pollution during haze events in China, Nature, 514, 218-222, 2014.

Smith, S. R., Bourassa, M. A., and Sharp, R. J.: Establishing more truth in true winds, J. Atmos. Ocean Tec., 16, 939-952, 1999.

Wu, D., Zhang, F., Lou, W., Li, D., and Chen, J.: Chemical characterization and toxicity assessment of fine particulate matters emitted from the combustion of petrol and diesel fuels, Sci. Tot. Environ., 605, 172-179, 2017.